



RADIATION EMITTED BY A CONSTANT LOAD IN A CIRCULAR MOTION ON AN ELASTICALLY SUPPORTED MINDLIN PLATE

A. V. KONONOV AND R. DE BORST

Faculty of Aerospace Engineering, Engineering Mechanics, TU Delft, The Netherlands.

E-mail: a.kononov@lr.tudelft.nl

(Received 23 June 2000, and in final form 10 November 2000)

Wave radiation is studied which is due to a constant load moving with a constant speed along a circular path over an unbounded Mindlin plate on a Winkler foundation. The steady state solution of the problem is obtained, showing that the radiation of elastic waves occurs for all non-zero load velocities. It is shown that the elastic wave field radiated by the supercritically moving load is confined in a spiral-like apex. The plate displacements at the boundaries of this apex are discontinuous. The radiated energy per period of load rotation is calculated as showing a discrete energy spectrum. For increasing load velocities, the total amount of radiated energy becomes larger. It is also shown that the major part of the radiated energy follows the direction of the load motion.

© 2001 Academic Press

1. INTRODUCTION

In the branch of mechanics which is devoted to the study of the dynamic processes which occur due to an interaction of moving objects with elastic structures a certain culture of knowledge and terminology has been established. Elastic wave radiation generated as a result of the interaction can be subdivided into a few basic types: Mach radiation (analogous to Vavilov–Cherenkov radiation in electrodynamics), transition radiation, diffraction radiation and radiation due to a non-uniformly moving source [1–4]. Most of these terms were originally generated in electrodynamics, where the need for the study of radiation due to moving sources (charged particles) was apparent much earlier than in mechanics.

It is known that a non-uniformly moving source of excitations radiates waves into a system [5]. Within the wide set of non-uniform source motions, a uniform motion along a circle can be considered as the simplest one. Indeed, in this motion, the velocity vector of an object changes its direction, but its value remains unaltered. The radiation emitted during such a motion possesses various specific features that clearly distinguish it from the basic radiation types mentioned above.

In the present paper, the radiation which is emitted by a constant load moving with a constant speed along a circle on an elastically supported Mindlin plate is studied. This model is not a restriction, since the approach can be applied to different models of elastic systems including three-dimensional systems. Fortunately, the main characteristics of the radiation can be analyzed analytically, e.g., spectra of radiated energy can be obtained in closed form.

Moreover, there is an analogy with cyclotron radiation of electromagnetic waves in electrodynamics. The cyclotron radiation was discovered experimentally in a cyclic particle accelerator 1947 [6]. Nowadays, cyclotron radiation is understood in a broad sense as radiation that is generated by a source of excitations, which moves along a circular path. In fact, this definition is applicable to fields of any physical nature [7]. Therefore, the present type of elastic wave radiation can, in some sense, be considered as cyclotron radiation in mechanics.

In the first part of the paper, the steady state behaviour of a plate due to a uniformly rotating load is determined in order to visualize the radiation process. In the second part, the radiated energy per period of load rotation and the energy spectra are derived and analyzed for different load velocities. Finally, the properties and the possible application of the radiation in mechanics are discussed.

2. MODEL

An unbounded plate (Mindlin plate) is considered with mass density ρ and flexural stiffness $D = Ed^3/(12(1 - \eta^2))$ $\{E, \text{Young's modulus}; \eta, \text{the Poisson ratio}; d, \text{thickness of the plate}\}$, resting on an elastic foundation with stiffness κ . The plate is subjected to constant load \tilde{P} , which moves with a constant angular velocity $\tilde{\Omega} = v/\tilde{r}_0$ along a circle with radius \tilde{r}_0 , see Figure 1 ($v = |\mathbf{V}|$ is the load velocity).

The dimensionless equations describing the motion of the system are [8]

$$\psi_{,tt}^x - \alpha^2(\psi_{,xx}^x + m\psi_{,yy}^x + p\psi_{,xy}^x) + \gamma(\psi^x - U_{,x}) = 0, \quad (1)$$

$$\psi_{,tt}^y - \alpha^2(\psi_{,yy}^y + m\psi_{,xx}^y + p\psi_{,xy}^y) + \gamma(\psi^y - U_{,y}) = 0, \quad (2)$$

$$U_{,tt} - (U_{,xx} + U_{,yy} - \psi_{,x}^x - \psi_{,y}^y) + U = -P\delta(x - r_0 \cos(\Omega t))\delta(y - r_0 \sin(\Omega t))$$

$$(-\infty < x, y < \infty, -\infty < t < \infty), \quad |U(x, y, t)| \rightarrow 0 \quad \text{as } r = \sqrt{x^2 + y^2} \rightarrow \infty, \quad (3)$$

where $\psi^x(x, y, t)$ and $\psi^y(x, y, t)$ are the local rotations in the x and y directions respectively, $U(x, y, t)$ is the transverse displacement of the plate, and P is the magnitude of the load. These dimensionless variables and parameters in equations (1)–(3) are introduced according

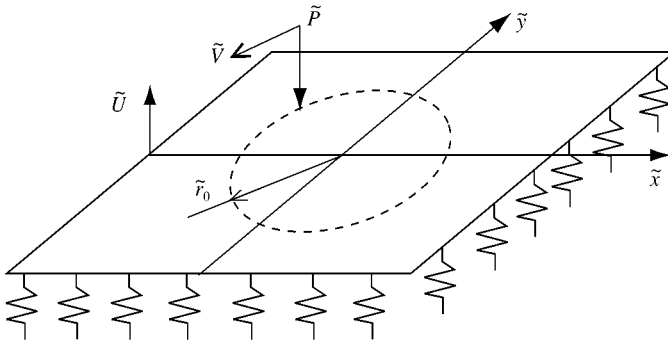


Figure 1. Model and reference system.

to the following definitions (the dimensional quantities are marked by \sim)

$$\begin{aligned}\{x, y, r_0\} &= \{\tilde{x}, \tilde{y}, \tilde{r}_0\}(\omega_0/c_{0t}), \quad t = \tilde{t}\omega_0, \quad U = \tilde{U}(\omega_0/c_{0t}), \quad \omega_0 = \sqrt{\kappa/\rho d}, \quad \alpha = c_1/c_{0t}, \\ m &= (1 - \eta)/2, \quad p = (1 + \eta)/2, \quad P = \tilde{P}\omega_0/\rho d c_{0t}^3, \quad \Omega = \beta/r_0, \quad \beta = v/c_{0t}, \\ c_1 &= \sqrt{E/\rho(1 - \eta^2)}, \quad c_t = \sqrt{\mu/\rho}, \quad c_{0t} = \sqrt{\chi}c_t, \quad \gamma = 6c_{0t}^2/\omega_0^2 d^2,\end{aligned}$$

where ω_0 is the eigenfrequency of the plate on an elastic foundation, α is the ratio between the compressional and modified shear wave velocities, c_1 and c_{0t} are compressional and shear wave velocities, μ is the shear modulus of the plate material, and χ is the numerical coefficient related to Mindlin's plate theory.

3. STEADY STATE SOLUTION TO THE PROBLEM

Application of the following Fourier transform over plane spatial co-ordinates

$$\{\psi_{\mathbf{k}}^x, \psi_{\mathbf{k}}^y, U_{\mathbf{k}}(k_1, k_2, t)\} = \iint \{\psi^x, \psi^y, U(x, y, t)\} \exp(-ik_1x - ik_2y) dx dy \quad (4)$$

to the system of equations (1)–(3), results in the system of ordinary differential equations with respect to time:

$$\psi_{\mathbf{k},tt}^x + \alpha^2(k_1^2 + mk_2^2 + \gamma)\psi_{\mathbf{k}}^x + \alpha^2pk_1k_2\psi_{\mathbf{k}}^y - \gamma ik_1U_{\mathbf{k}} = 0, \quad (5)$$

$$\psi_{\mathbf{k},tt}^y + \alpha^2(k_2^2 + mk_1^2 + \gamma)\psi_{\mathbf{k}}^y + \alpha^2pk_1k_2\psi_{\mathbf{k}}^x - \gamma ik_2U_{\mathbf{k}} = 0, \quad (6)$$

$$U_{\mathbf{k},tt} + (k_1^2 + k_2^2 + 1)U_{\mathbf{k}} + ik_1\psi_{\mathbf{k}}^x + ik_2\psi_{\mathbf{k}}^y = -P \exp(-ik_1r_0 \cos(\Omega t) - ik_2r_0 \sin(\Omega t)). \quad (7)$$

Using the following relation:

$$\exp(-iz \cos(\theta)) = \sum_{n=-\infty}^{\infty} (-i)^n J_n(z) \exp(in\theta)$$

with $J_n(z)$ the Bessel function of the first kind, the exponent in the right part of equation (7) can be expanded into an infinite series as follows:

$$\begin{aligned}\exp(-ik_1r_0 \cos(\Omega t) - ik_2r_0 \sin(\Omega t)) \\ \Rightarrow = \exp(-ikr_0 \cos(\varphi_k - \Omega t)) = \sum_{n=-\infty}^{\infty} (-i)^n J_n(kr_0) \exp(in(\varphi_k - \Omega t)),\end{aligned} \quad (8)$$

where $k = \sqrt{k_1^2 + k_2^2}$ and $k_1 = k \cos(\varphi_k)$, $k_2 = k \sin(\varphi_k)$. A solution to the linear system (equations (5)–(7)) with the modified right part (equation (8)), can be presented as a sum, where each term is a solution of the system

$$\psi_{n\mathbf{k},tt}^x + \alpha^2(k_1^2 + mk_2^2 + \gamma)\psi_{n\mathbf{k}}^x + \alpha^2pk_1k_2\psi_{n\mathbf{k}}^y - \gamma ik_1U_{n\mathbf{k}} = 0,$$

$$\psi_{n\mathbf{k},tt}^y + \alpha^2(k_2^2 + mk_1^2 + \gamma)\psi_{n\mathbf{k}}^y + \alpha^2pk_1k_2\psi_{n\mathbf{k}}^x - \gamma ik_2U_{n\mathbf{k}} = 0,$$

$$U_{n\mathbf{k},tt} + (k_1^2 + k_2^2 + 1)U_{n\mathbf{k}} + ik_1\psi_{n\mathbf{k}}^x + ik_2\psi_{n\mathbf{k}}^y = -P(-i)^n J_n(kr_0) \exp(in(\varphi_k - \Omega t)).$$

Substitution of a partial solution of the form

$$\{\psi_{nk}^x, \psi_{nk}^y, U_{nk}\} = \{A_n, B_n, C_n\} \exp(-in\Omega t)$$

into this system, results in a linear algebraic system with respect to unknowns $\{A_n, B_n, C_n\}$. After solution of this system, C_n (note that A_n, B_n are given in Appendix B since we are merely interested in the plate displacement) becomes

$$C_n = \frac{-P(-i)^n J_n(kr_0)(\alpha^2 k^2 - (n\Omega)^2 + \gamma)}{(k^2 - (n\Omega)^2 + 1)(\alpha^2 k^2 - (n\Omega)^2 + \gamma) - \gamma k^2}.$$

Then for U_{nk} :

$$U_{nk}(k, \varphi_k, t) = \frac{-P(-i)^n J_n(kr_0)(\alpha^2 k^2 - (n\Omega)^2 + \gamma)}{((k^2 - (n\Omega)^2 + 1)(\alpha^2 k^2 - (n\Omega)^2 + \gamma) - \gamma k^2)} \exp(in(\varphi_k - \Omega t)). \quad (9)$$

$U_{nk}(k, \varphi_k, t)$ depends on the magnitude of the wave vector k and its direction. Thus, the inverse operator for the Fourier transform (4) in a polar system of co-ordinates in the k -space can be rewritten as

$$U(r, \varphi, t) = \frac{1}{4\pi^2} \int_0^\infty \int_0^{2\pi} k U_{\mathbf{k}}(k, \varphi_k, t) \exp(ikr \cos(\varphi_k - \varphi)) d\varphi_k dk \quad (10)$$

using the following definitions:

$$\mathbf{k} = (k_1, k_2) = (k \cos(\varphi_k), k \sin(\varphi_k)), \quad \mathbf{r} = (x, y) = (r \cos(\varphi), r \sin(\varphi)).$$

Application of transform (10) to expression (9) and using the substitution

$$\varphi_k = \eta + \varphi + \frac{\pi}{2} \Rightarrow d\varphi_k = d\eta$$

and the integral representation of Bessel functions of the first kind [9]

$$J_n(kr) = \frac{1}{2\pi} \int_0^{2\pi} \exp((in\eta - kr \sin(\eta))) d\eta$$

yields

$$U_n(r, \varphi, t) = \frac{-P}{2\pi} \int_0^\infty \frac{k(\alpha^2 k^2 - (n\Omega)^2 + \gamma) J_n(kr_0) J_n(kr)}{((k^2 - (n\Omega)^2 + 1)(\alpha^2 k^2 - (n\Omega)^2 + \gamma) - \gamma k^2)} \exp(in(\varphi - \Omega t)) dk \quad (11)$$

and the total transverse displacement of the plate is given by the sum

$$U(r, \varphi, t) = \sum_{n=-\infty}^{\infty} U_n(r, \varphi, t). \quad (12)$$

The integral in equation (11) can be elaborated analytically employing certain properties of Bessel function [9], as follows for $n \geq 0$ and < 0 respectively:

$$I_n^* = \int_0^\infty \frac{kh(k)J_n(kr_0)J_n(kr)}{g(k)} dk = \begin{cases} \sum_{\kappa=k_{(l)n}^*}^{l=L} \pi i \frac{\kappa h(\kappa)}{dg(\kappa)/d\kappa} J_n(\kappa r) H_n^{(1)}(\kappa r_0), & r \leq r_0, \\ \sum_{\kappa=k_{(l)n}^*}^{l=L} \pi i \frac{\kappa h(\kappa)}{dg(\kappa)/d\kappa} J_n(\kappa r_0) H_n^{(1)}(\kappa r), & r_0 < r \end{cases} \quad (13)$$

with $k_{(l)n}^*$: $g(k_{(l)n}^*) = 0$, and L is the number of roots with $\text{Im}(k_l^*) \geq 0$:

$$I_n^* = \int_0^\infty \frac{kh(k)J_n(kr_0)J_n(kr)}{g(k)} dk = \begin{cases} - \sum_{\kappa=k_{(j)n}^*}^{j=J} \pi i \frac{\kappa h(\kappa)}{dg(\kappa)/d\kappa} J_n(\kappa r) H_n^{(2)}(\kappa r_0), & r \leq r_0 \\ - \sum_{\kappa=k_{(j)n}^*}^{j=J} \pi i \frac{\kappa h(\kappa)}{dg(\kappa)/d\kappa} J_n(\kappa r_0) H_n^{(2)}(\kappa r), & r_0 \leq r \end{cases}$$

with $k_{(j)n}^*$: $g(k_{(j)n}^*) = 0$, and J is the number of roots with $\text{Im}(k_j^*) < 0$. Here $H_n^{(1,2)}$ are Hankel functions and

$$h(k) = \alpha^2 k^2 - (n\Omega)^2 + \gamma, \quad g(k) = (k^2 - (n\Omega)^2 + 1)(\alpha^2 k^2 - (n\Omega)^2 + \gamma) - \gamma k^2.$$

The result (equation (13)) has been obtained taking into account that the total solution should only consist of outgoing waves (waves travelling from the source of disturbances towards infinity) and using asymptotic expressions for the Hankel functions for large arguments [9]

$$H_n^{(1,2)}(k_n r) \approx \sqrt{\frac{2}{\pi k_n r}} \exp\left(\pm i\left(k_n r - \frac{\pi n}{2} - \frac{\pi}{4}\right)\right) \quad \text{as } k_n r \rightarrow \infty,$$

Thus, for $n \geq 0$ in I^* the term with $H_n^{(1)}(k^* r)$ and $\text{Im}(k^*) > 0$ should be taken, whilst, for $n < 0$ the term with $H_n^{(2)}(kr)$ and $\text{Im}(k^*) < 0$ should be taken. Finally, the terms with negative and positive indices can be combined together taking into account that for periodic real-valued function $F(z)$ expanded into Fourier series the following symmetry relations hold:

$$F(z) = \sum_{n=-\infty}^{\infty} f_n \exp(i\Delta n z) \Rightarrow \text{Re}(f_n) = \text{Re}(f_{-n}), \quad \text{Im}(f_n) = -\text{Im}(f_{-n})$$

So, for the steady state plate displacement

$$U(r, \varphi, t) = -\frac{P}{2\pi} \sum_{n=0}^{\infty} \varepsilon_n (\cos(n(\varphi - \Omega t)) \text{Re}(\Gamma_n(r, t)) - \sin(n(\varphi - \Omega t)) \text{Im}(\Gamma_n(r, t))), \quad (14)$$

where

$$\varepsilon_n = \begin{cases} 1 & n = 0 \\ 2 & n > 0 \end{cases}$$

and

$$\Gamma_n(r, t) = \begin{cases} \sum_{\kappa=k_1^*}^{l=2} \frac{\pi i}{2} \frac{\alpha^2 \kappa^2 - (n\Omega)^2 + \gamma}{(\alpha^2 + 1)(n\Omega)^2 - 2\alpha^2 \kappa^2 - \alpha^2} J_n(\kappa r) H_n^{(1)}(\kappa r_0), & r \leq r_0, \\ \sum_{\kappa=k_1^*}^{l=2} \frac{\pi i}{2} \frac{\alpha^2 \kappa^2 - (n\Omega)^2 + \gamma}{(\alpha^2 + 1)(n\Omega)^2 - 2\alpha^2 \kappa^2 - \alpha^2} J_n(\kappa r_0) H_n^{(1)}(\kappa r), & r_0 \leq r \end{cases}$$

with the sum over $k_{(1)n}^*, k_{(2)n}^*$:

$$k_{(1,2)n}^* = \frac{1}{\sqrt{2\alpha}}$$

$$\sqrt{\alpha^2 (n\Omega)^2 - 1 + (n\Omega)^2 \pm \sqrt{4\alpha^2 ((n\Omega)^2 - 1)((n\Omega)^2 - \gamma) - (\alpha^2 ((n\Omega)^2 - 1) + (n\Omega)^2)^2}}.$$

In Figure 2 the results of the numerical calculations of the obtained solution, equation (14), are depicted for two different load velocities. Clearly, the load radiates elastic waves into the plate in both cases. It is also observed that for larger load velocities the radiation is more powerful. The form of equation (14) can also confirm the presence of the radiation for any non-zero velocity of the load. As is seen, the solution consists of a symmetric ($\cos(n(\varphi - \Omega t))$) and an asymmetric ($\sin(n(\varphi - \Omega t))$) with respect to the load, even in the absence of dissipation. This indicates that the reaction of the elastic system at the loading point is not vertical and has the longitudinal projection. Thus, a certain longitudinal force and, therefore, energy have to be applied constantly by the external source in order to maintain a uniform load motion. At large distances from the load, an ‘‘observer’’ registers a series of ‘‘pulses’’ at time intervals equal to the period of the load rotation $T = 2\pi/\Omega$, as it shown in Figure 3. It is noted that an oscillating tail, which results from the dispersion of the system, follows each pulse.

The longitudinal component \mathbf{f}_l can be calculated using for formula [1]

$$\mathbf{f}_l = (\mathbf{f}_r, \mathbf{f}_{l\varphi}) = -\frac{P}{2} (\nabla U(r, \varphi)|_{r=r_0+0, \varphi=\Omega t+0} + \nabla U(r, \varphi)|_{r=r_0-0, \varphi=\Omega t-0}). \quad (15)$$

The results of calculations are shown in Figure 4. From the figure it is seen that for the load velocities smaller than β_{cr} when the radiation is relatively weak, \mathbf{f}_l has two components ($\mathbf{f}_r, \mathbf{f}_{l\varphi}$) where rise in the angular component originated by wave pressure and the radial

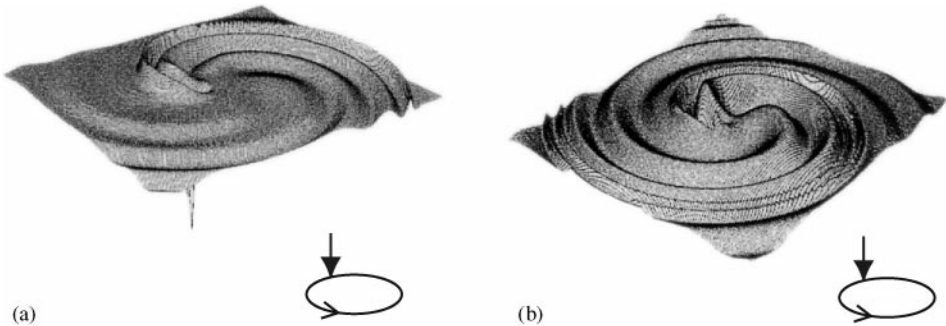


Figure 2. Plate displacements for two different load velocities: (a) $\beta = 0.9$ and (b) $\beta = 1.6$.

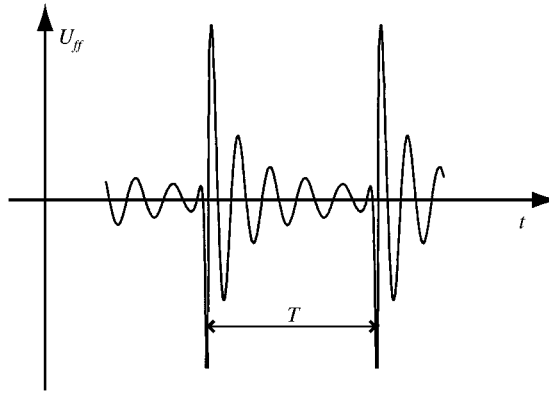


Figure 3. Time dependence of the “far-field” plate displacements.

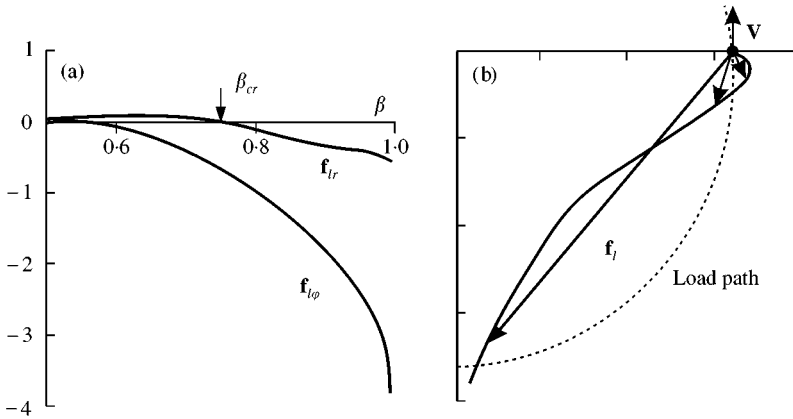


Figure 4. Longitudinal force acting on load: (a) graph of components, (b) vector representation.

component appears due to load rotation, where β_{cr} is the so-called critical velocity:

$$\beta_{cr} = \sqrt{\alpha^2 - \gamma(\alpha^2 + 2) + 2\gamma\sqrt{\alpha^2(\gamma - 1) + 1}/|\gamma - 1|},$$

which is defined by the fact that a rectilinearly and uniformly moving constant load radiates the elastic waves if its velocity is larger than β_{cr} . Further, for $\beta > \beta_{cr}$, when the radiation is more powerful, the radial component changes sign due to strong wave pressure.

4. ANALYSIS OF THE SOLUTION

It is well known that the elastic field generated by a rectilinearly moving load over some elastic system (for instance an elastically supported membrane or elastic half-space) is confined to a certain apex when it moves supercritically [10]. This apex is the two-dimensional image of a Mach cone in acoustics. On the border of such an apex the displacements of elastic system or its spatial derivatives can be discontinuous. The question thus arises whether similar discontinuity in displacements exists along a certain singular curve for the circular load motion. This question can be answered by analyzing the

divergence of $\partial U/\partial r$. However, the solution (equation (14)) written in the series form is not convenient for such an analysis. A relevant compact form of the solution can be obtained with the help of the fundamental solution method.

If the fundamental solution of the differential operator (equations (1)–(3)) is known, then the steady state vertical displacement of the plate is given by the convolution

$$U(x, y, t) = -P \lim_{t \rightarrow \infty} \int_{t'=0}^t \int_{-\infty}^{\infty} \int_{-\infty}^{\infty} G_u(|r-r'|, t-t') \delta(x' - r_0 \cos(\Omega t')) \times \delta(y' - r_0 \sin(\Omega t')) dx' dy' dt', \quad (16)$$

where $G_u(\cdot)$ is the fundamental solution, $|r-r'| = \sqrt{(x-x')^2 + (y-y')^2}$.

Integration over x' and y' in equation (16), using the property of the δ -function in convoluting integrals and introduction of a polar system of co-ordinates $x = r \cos(\varphi)$, $y = r \sin(\varphi)$ leads to

$$U(r, \varphi, t) = -P \lim_{t \rightarrow \infty} \int_{t'=0}^t G_u(\sqrt{r^2 + r_0^2 - 2rr_0 \cos(\varphi - \Omega t')}, t-t') dt'.$$

Further, introduction of a rotating co-ordinate system, $r = r$, $\eta = \varphi - \Omega t$, where the steady state originates, and new integration variable $\tau = t - t'$ allows the limit in equation (16) to be taken as

$$U(r, \eta) = -P \int_{\tau=0}^{\infty} G_u(\sqrt{r^2 + r_0^2 - 2rr_0 \cos(\eta + \Omega \tau)}, \tau) d\tau. \quad (17)$$

Thus, analyzing the singularities of the integrand in equation (17) an expression for the singular curves is found. For the Mindlin plate the fundamental solution can be written in the following dimensionless form (the details of this derivation are given in Appendix A):

$$G_u(r, t) = \frac{F_1(r, t)}{\sqrt{t^2 - r^2}} \theta(t - |r|) + F_2(r, t), \quad (18)$$

where $F_1(r, t)$ and $F_2(r, t)$ are smooth and “well-behaved” functions and $\theta(\cdot)$ is the Heaviside step-function. Thus, according to equation (17)

$$U(r, \eta) = -P \left\{ \int_0^{\infty} \frac{F_1(\sqrt{f(r, \eta, \tau)}, \tau)}{\sqrt{f(r, \eta, \tau)}} \theta(f(r, \eta, \tau)) d\tau + \int_0^{\infty} F_2(\sqrt{f(r, \eta, \tau)}, \tau) d\tau \right\}$$

with $f(r, \eta, \tau) = \tau^2 - r^2 - r_0^2 + 2rr_0 \cos(\eta + \Omega \tau)$. From this expression it is seen that the sufficient condition for the plate displacement discontinuities is that the equation

$$f(r, r_0, \tau) = \tau^2 - r^2 - r_0^2 + 2rr_0 \cos(\eta + \Omega \tau) = 0$$

has a real double root with respect to τ . This implies that the following system of equations should be satisfied:

$$f(R, \eta, \xi) = a^2 \xi^2 - R^2 - 1 + 2R \cos(\eta + \xi) = 0, \quad (19a)$$

$$\frac{\partial f(R, \eta, \xi)}{\partial \xi} = 2a^2 \xi - 2R \sin(\eta + \xi) = 0, \quad (19b)$$

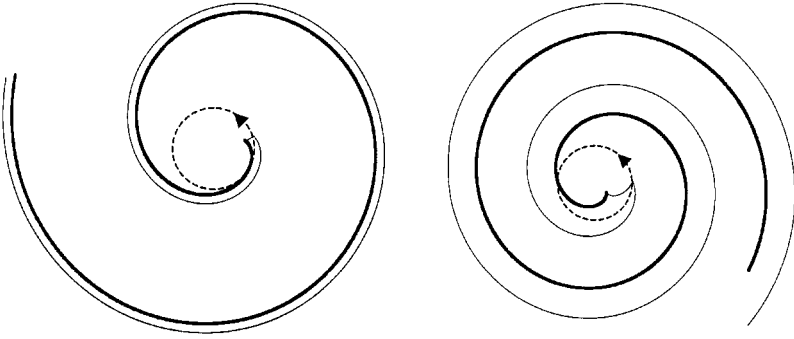


Figure 5. Singular curves for two different supercritical load velocities: (a) $\beta = 1.2$, (b) $\beta = 2.5$.

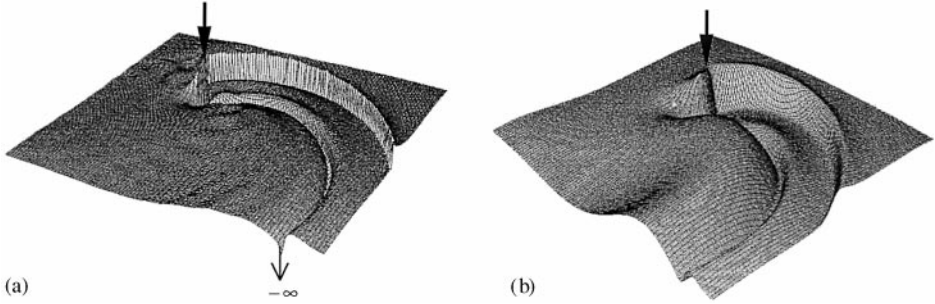


Figure 6. Plate displacements near the point load, (a) without and (b) with internal friction in the plate.

where $R = r/r_0$, $\xi = \Omega\tau$ and $a = 1/\beta = c_{0t}/v$. The system of equation (19) can have a solution if the following relations between η and R hold:

$$\eta_{1,2} = -\frac{1}{a}(\sqrt{R^2 - a^2} \mp \sqrt{1 - a^2}) + \arccos\left(\frac{a^2 \pm \sqrt{R^2 - a^2} \sqrt{1 - a^2}}{R}\right). \quad (20)$$

An analysis of equation (20) shows that the relations between η and R describe a certain singular curve (which consists of two parts η_1 and η_2) on the plate if the parameters are taken as follows: $a < 1 \Rightarrow v > c_{0t} \vee R \geq a \Rightarrow r \geq r_0 v/c_{0t}$, i.e., such a curve exists when the load moves supercritically. In Figure 5, two such singular curves are depicted for different supercritical load velocities. The thin line denotes η_1 , the thick line denotes η_2 and the dashed line represents the path of the load respectively.

It is observed that the radiated field is bounded by a spiral-like apex, whose vertex coincides with the instantaneous load position. At large distances from the load ($R \rightarrow \infty$) the sides of the cone approach a simple spiral form, which can be approximated as $R \sim \beta\eta_{1,2}$. Further analysis shows that along η_1 the plate displacements exhibit a jump and along η_2 the displacements tend to infinity ($-\infty$). This divergence of the displacements can be considered as a “bad feature” of the model and it can be avoided (as physically non-realistic) by taking into consideration, for example, the internal friction in the plate material (as it is shown in Figure 6(b)).

A qualitative geometrical interpretation of the system of equation (19) given as follows. Equation (19a) describes the geometrical position of the set of successive circular wave

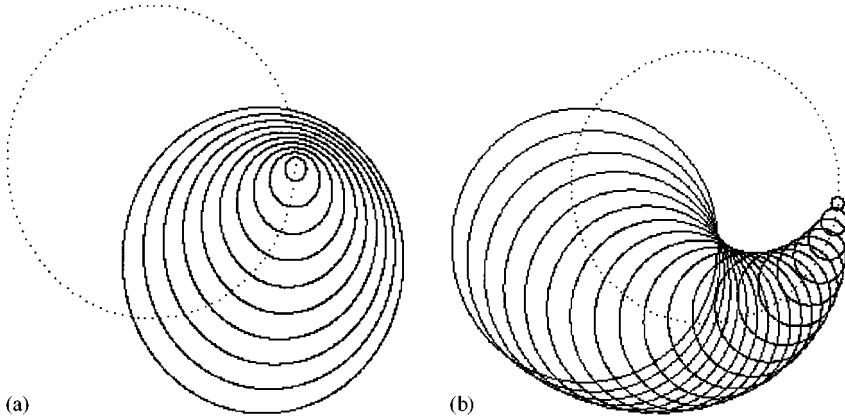


Figure 7. Set of successive circular wave fronts moving out from successive positions of a load, with moves (a) subcritically, (b) supercritically.

fronts with radius $a\xi$ emitted by the point-like source at the times ξ , which moves with unit angular velocity along a unit circle (see Figure 7).

This parametric set of the circles either has a common envelope or a tangential curve, if load moves supercritically (see Figure 7(b)). An explicit or an implicit equation for the tangential curve can be found by solving the system of equations (19). Evidently, along the tangential curve, the wave fronts emitted by a moving source of disturbances at the successive moments of time superpose in-phase to produce a “shock” front. In a 2-D case for the models with a limited wave velocity, this leads to a discontinuity of the displacement along the tangential curve, as shown in Figure 6. In the problem under consideration, such a “shock” front implies a discontinuity of the displacements of the plate near the tangential curve.

5. ENERGY SPECTRUM

As can be deduced from equation (9), the rotating load radiates a discrete frequency spectrum with the frequencies ω_n proportional to the angular frequency of the load rotation $\omega_n = n\Omega$ with $n > n^* = \sqrt{\gamma/\Omega}$ and corresponding wave numbers $k_n = k_{(1,2)n}^*$, where harmonics with $n > n^*$ describe the propagating waves since for such n wave numbers are real-valued. In order to study the energy characteristics of the radiation, the radiated energy per period of the load rotation E_T is analyzed. This amount of energy is given by the sum

$$E_T = \sum_{n > n^*}^{\infty} E_n, \quad (21)$$

where E_n is the energy carried away by the n th harmonic of the far field U_n^R ($r \gg r_0$) that represents the so-called wave field. To this end, the energy density flux of the n th harmonic through a circle around the origin with a large radius r : ($r \gg r_0$) for one period $T = 2\pi/\Omega$ of the load rotation [11], is

$$E_n = \lim_{r \rightarrow \infty} \frac{1}{T} \int_{t=0}^T \int_{\varphi=0}^{2\pi} (\mathbf{S}_n, \hat{\mathbf{r}}) r d\varphi d\tau \quad \text{for } n > n^*, \quad (22)$$

where (\cdot, \cdot) denotes the scalar product. The density of the energy flux \mathbf{S}_n in equation (22) is given by (for a derivation of \mathbf{S}_n the reader is referred to Appendix B)

$$\mathbf{S}_n \approx -\rho c_{0t}^3 \frac{\partial U_n^R}{\partial \tau} \left(\hat{r} \frac{\partial U_n^R}{\partial r} + \hat{\phi} \frac{1}{r} \frac{\partial U_n^R}{\partial \phi} \right),$$

where \hat{r} and $\hat{\phi}$ are unit vectors. Using this expression the scalar product in the integrand of equation (22) can be elaborated to give the r -component of the energy flux

$$(\mathbf{S}_n, \hat{r}) = S_n^r = -\rho c_{0t}^3 \frac{\partial U_n^R}{\partial \tau} \frac{\partial U_n^R}{\partial r}. \quad (23)$$

Substituting the n th harmonic of the far (or wave) field which is derived from equation (14)

$$U_n^R(r, \phi, t) = U_n^{R1}(r, \phi, t) + U_n^{R2}(r, \phi, t),$$

with

$$U_n^{R1} = -PG_{(1)n}(\Omega) J_n(k_{(1)n}^* r_0) (\sin(n(\phi - \Omega\tau)) J_n(k_{(1)n}^* r) + \cos(n(\phi - \Omega\tau)) Y_n(k_{(1)n}^* r)),$$

$$U_n^{R2} = -PG_{(2)n}(\Omega) J_n(k_{(2)n}^* r_0) (\sin(n(\phi - \Omega\tau)) J_n(k_{(2)n}^* r) + \cos(n(\phi - \Omega\tau)) Y_n(k_{(2)n}^* r)),$$

and

$$G_{(1,2)n}(\Omega) = \frac{(\alpha^2 - 1)(n\Omega)^2 - \alpha^2 + 2\gamma \pm D_n}{2D_n},$$

$$D_n = \sqrt{4\alpha^2((n\Omega)^2 - 1)(n\Omega)^2 - \gamma) - (\alpha^2((n\Omega)^2 - 1) + (n\Omega)^2)^2}$$

into equation (23) and taking into account only those members which are decreasing for large r inversely proportional to r gives (the “wave zone” [7] is considered)

$$S_n^r(r, \phi) = A_1 S_n^{r1}(r, \phi) + A_2 S_n^{r2}(r, \phi),$$

$$S_n^{r1}(r, \phi) = \sin^2(n(\phi - \Omega\tau)) \frac{2}{\pi k_{(1)n}^* r} - \cos(2n(\phi - \Omega\tau)) J_n(k_{(1)n}^* r) Y_{n+1}(k_{(1)n}^* r),$$

$$S_n^{r2}(r, \phi) = \sin^2(n(\phi - \Omega\tau)) \frac{2}{\pi k_{(2)n}^* r} - \cos(2n(\phi - \Omega\tau)) J_n(k_{(2)n}^* r) Y_{n+1}(k_{(2)n}^* r), \quad (24)$$

where $A_1 = \rho c_{0t}^3 n\Omega k_{(1)n}^* (PG_{(1)n}(\Omega) J_n(k_{(1)n}^* r_0))^2$, $A_2 = \rho c_{0t}^3 n\Omega k_{(2)n}^* (PG_{(2)n}(\Omega) J_n(k_{(2)n}^* r_0))^2$.

From this expression, it follows that for $\phi - \Omega\tau = \pi/2$, S_n^r attains a maximum. Physically, it means that the energy flux reaches a maximum when a vector \mathbf{r} that is pointed in the direction of an “observer” is parallel to the load velocity vector as depicted in Figure 8. In other words, the largest part of the radiated energy follows the direction of the load motion.

Finally, the expression for S_n^r (equation (24)) is substituted into equation (22). After integration this results in the energy carried away by the n th harmonic of the radiated wave field

$$E_n = \rho c_{0t}^3 P^2 n\Omega (G_{(1)n}^2 J_n^2(k_{(1)n}^* r_0) + G_{(2)n}^2 J_n^2(k_{(2)n}^* r_0)). \quad (25)$$

This result is depicted in Figure 9. Since the motion is periodic, the energy spectrum is discrete. The total amount of radiated energy per load period using equations (21) and (25) can be calculated numerically. For velocities of the load smaller than the wave velocity ($\beta < 1$) it is seen that with increasing load velocity the maximum of the energy spectrum shifts towards harmonics of higher order and that the total amount of radiated energy

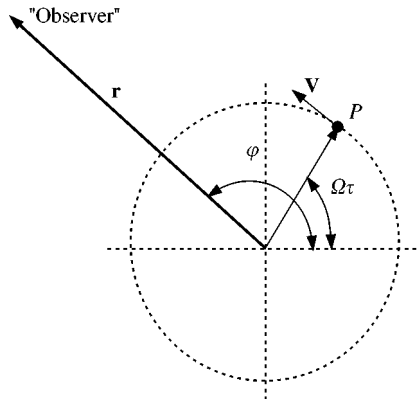


Figure 8. Load mainly radiates in the direction of its velocity.

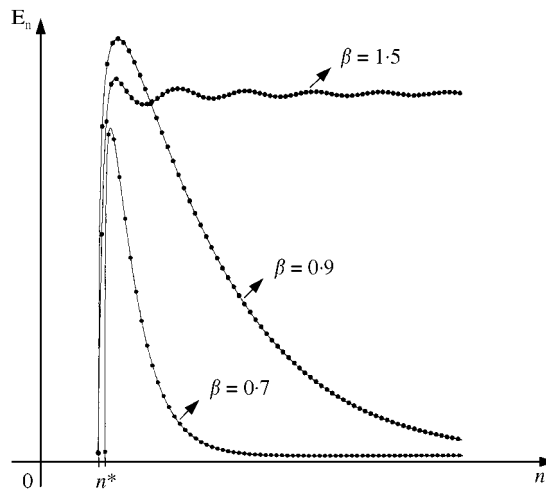


Figure 9. Energy spectra for three different load velocities.

becomes larger, but remains finite. Theoretically, it is possible to obtain the radiation maximum for very high frequencies by varying the frequency of the load rotations. For supercritical load velocities ($\beta > 1$) the total amount of radiated energy is infinite. Indeed, in the previous Section it has been shown that when the load moves supercritically ($\beta > 1$) the plate displacement is discontinuous along a certain curve. Thus, it follows that the power radiation should be infinite.

6. CONCLUSIONS

In this paper, the elastic wave radiation which is due to a constant load moving with a constant speed along a circular path over an unbounded Mindlin plate on a Winkler foundation has been investigated. The complete steady state solution of the problem has been obtained. It has been shown that for all velocities the load radiates elastic waves into the plate. This radiation is analogous to the cyclotron radiation in electrodynamics. From

an analysis of the plate displacements, is shown that the elastic field radiated by the supercritically moving load is confined in a spiral-like apex. The plate displacements at the boundaries of this apex are discontinuous. Further, the radiated energy per period of load rotation has been calculated as displaying a discrete energy spectrum. It has been shown that for increasing load velocities the total amount of radiated energy becomes larger. The major part of the radiated energy follows the direction of the load motion. The principal conclusions and the radiation phenomenon are also valid for the other plate models, since a load, which is moving non-uniformly over a structure, emits the waves.

Finally, possible applications of the radiation in mechanics are discussed. The analysis shows that the radiation possesses certain properties that can be used in devices for a non-destructive inspection. In particular, the following properties are to be underlined:

Direction of the radiation: the radiated energy is mainly concentrated inside the narrow cone, which has been described in section 4. Therefore, it can be concluded that the radiation is concentrated inside the narrow beam or, in other words, the radiation is directed;

Scanning function: due to uniform rotation of the load and, consequently the radiation cone the scanning function is automatically realized, since the radiation beam passes once through each point of the outside area during one period of the load rotation;

Certain frequency spectrum of the radiation: a spectrum of the radiation is predefined by the frequency of the load rotation. The corresponding discrete energy spectrum has a clearly expressed maximum with a location that can be controlled by the rate of the load velocity. It is theoretically seen that this maximum can be shifted to the ultrasonic range of frequencies.

The majority of non-destructive inspection techniques are based on the wave scattering phenomenon. This means that information on the specimen condition can be obtained by analyzing a wave field scattered by the specimen. The irradiating wave field is generated by some transducer (usually an ultrasonic one). However, a circularly moving source of excitations that has been analyzed, without specifying its physical nature, can play a role of such an elementary transducer.

REFERENCES

1. A. VESNITSKI and A. METRIKINE 1996 *Soviet Physics Uspekhi* **39**, 983–1007. Transition radiation in mechanics.
2. A. WOLFERT, A. METRIKINE and H. DIETERMAN, 1996 *Wave Motion* **24**, 185–196. Wave radiation in a one-dimensional system due to a non-uniformly moving constant load.
3. A. KONONOV and A. METRIKINE 1996 *Mechanics of Solids (Izvestiya Akademii Nauk SSR, Mekhanika Tverdogo Tela)* **31**, 44–48. A diffractive radiation in two-dimensional elastic systems.
4. A. S. J. SUIKER, R. DE BORST, C. ESVELD 1988 *Archives of Applied Mechanics* **68**, 158–168. Critical behaviour of a Timoshenko beam-half plane system under a moving load.
5. SMITH, S. GLENN 1997 *An introduction to classical electromagnetic radiation*. Cambridge, UK: Cambridge University Press.
6. J. D. JACKSON 1975 *Classical Electrodynamics*. New York: Wiley.
7. V. GINZBURG 1979 *Theoretical Physics and Astrophysics*. Oxford: Pergamon.
8. J. ACHENBACH 1993 *Wave Propagation in Elastic Solids*. Amsterdam: North-Holland; seventh edition.
9. G. WATSON 1996 *A treatise on the Theory of Bessel Functions*. Cambridge: Cambridge University Press.
10. L. SCHWARTZ 1967 *Mathematics of Physical Sciences*. New York: Addison-Wesley.
11. P. MORSE and H. FRESHBACH 1953 *Methods of Theoretical Physics*. New York: McGraw-Hill Book Company.

APPENDIX A: FUNDAMENTAL SOLUTION FOR MINDLIN PLATE

The fundamental solution $G_u(\cdot)$ of differential operator of problem (1)–(3) can be found from the system

$$\psi_{,tt}^x - \alpha^2(\psi_{,xx}^x + m\psi_{,yy}^x + p\psi_{,xy}^y) + \gamma(\psi^x - G_{u,x}) = 0, \quad (\text{A.1})$$

$$\psi_{,tt}^y - \alpha^2(\psi_{,yy}^y + m\psi_{,xx}^y + p\psi_{,xy}^x) + \gamma(\psi^y - G_{u,y}) = 0, \quad (\text{A.2})$$

$$G_{u,tt} - (G_{u,xx} + G_{u,yy} - \psi_{,x}^x - \psi_{,y}^y) + G_u = \delta(x)\delta(y)\delta(t) \quad (-\infty < x, y < \infty, 0 \leq t),$$

$$|G_u(x, y, t)| \rightarrow 0 \quad \text{as } r = \sqrt{x^2 + y^2} \rightarrow \infty. \quad (\text{A.3})$$

By employing the following Fourier transform over plane spatial co-ordinates

$$\{\tilde{\psi}^x, \tilde{\psi}^y, \tilde{G}_u(k_1, k_2, t)\} = \iint \{\psi^x, \psi^y, G_u(x, y, t)\} \exp(-ik_1x - ik_2y) dx dy \quad (\text{A.4})$$

in combination with the Laplace transform over time

$$\{\hat{\tilde{\psi}}^x, \hat{\tilde{\psi}}^y, \hat{\tilde{G}}_u(k_1, k_2, p)\} = \int_0^\infty \{\tilde{\psi}^x, \tilde{\psi}^y, \tilde{G}_u(k_1, k_2, t)\} \exp(-pt) dt$$

system (A.1)–(A.3) reduces to the algebraic system

$$p^2 \hat{\tilde{\psi}}^x + \alpha^2(k_1^2 + mk_2^2 + \gamma) \hat{\tilde{\psi}}^x + \alpha^2 pk_1 k_2 \hat{\tilde{\psi}}^y - \gamma ik_1 \hat{\tilde{G}}_u = 0,$$

$$p^2 \hat{\tilde{\psi}}^y + \alpha^2(k_2^2 + mk_1^2 + \gamma) \hat{\tilde{\psi}}^y + \alpha^2 pk_1 k_2 \hat{\tilde{\psi}}^x - \gamma ik_2 \hat{\tilde{G}}_u = 0,$$

$$p^2 \hat{\tilde{G}}_u + (k_1^2 + k_2^2 + 1) \hat{\tilde{G}}_u + ik_1 \hat{\tilde{\psi}}^x + ik_2 \hat{\tilde{\psi}}^y = 1.$$

The solution of this system with respect to $\hat{\tilde{G}}_u$ is

$$\hat{\tilde{G}}_u(k_1, k_2, p) = \frac{(p^2 + \alpha^2 k^2 + \gamma)}{(p^2 + k^2 + 1)(p^2 + \alpha^2 k^2 + \gamma) - \gamma k^2}. \quad (\text{A.5})$$

Further, inversion of the Laplace transform results in

$$\begin{aligned} \tilde{G}_u(k_1, k_2, t) = & \frac{(\alpha^2 k^2 + \gamma) - (k^2 + 1) + \sqrt{D}}{\sqrt{D} K_1} \sin(t K_1) \\ & - \frac{(\alpha^2 k^2 + \gamma) - (k^2 + 1) - \sqrt{D}}{\sqrt{D} K_2} \sin(t K_2), \end{aligned} \quad (\text{A.6})$$

where

$$K_1 = \frac{1}{\sqrt{2}} \sqrt{\alpha^2 k^2 + \gamma + k^2 + 1 - \sqrt{D}}, \quad K_2 = \frac{1}{\sqrt{2}} \sqrt{\alpha^2 k^2 + \gamma + k^2 + 1 + \sqrt{D}}$$

and

$$D = ((\alpha^2 k^2 + \gamma) - (k^2 + 1))^2 + 4k^2\gamma, \quad k^2 = k_1^2 + k_2^2.$$

It is useful to rewrite the inverse operator for the Fourier transform (A.4) into polar system of co-ordinates

$$G_u(r, \varphi, t) = \frac{1}{4\pi^2} \int_0^\infty \int_0^{2\pi} k \tilde{G}_u(k, \varphi_k, t) \exp(ikr \cos(\varphi_k - \varphi)) d\varphi_k dk. \quad (\text{A.7})$$

Substitution of equation (A.6) into (A.7) and subsequent integration over φ_k gives

$$G_u(r, t) = G_u^t(r, t) + G_u^l(r, t),$$

where

$$G_u^t(r, t) = + \frac{1}{2\pi} \int_0^\infty k \frac{(\alpha^2 k^2 + \gamma) - (k^2 + 1) + \sqrt{D(k)}}{\sqrt{D(k)} K_1(k)} J_0(kr) \sin(tK_1(k)) dk, \quad (\text{A.8})$$

$$G_u^l(r, t) = - \frac{1}{2\pi} \int_0^\infty k \frac{(\alpha^2 k^2 + \gamma) - (k^2 + 1) + \sqrt{D(k)}}{\sqrt{D(k)} K_2(k)} J_0(kr) \sin(tK_2(k)) dk. \quad (\text{A.9})$$

Equations (A.8) and (A.9) can be rewritten in the approximate form as follows:

$$\begin{aligned} G_u^t(r, t) &\approx \frac{1}{2\pi} \int_0^A k \frac{(\alpha^2 k^2 + \gamma) - (k^2 + 1) + \sqrt{D(k)}}{\sqrt{D(k)} K_1(k)} J_0(kr) \sin(tK_1(k)) dk \\ &\quad + \frac{1}{\pi} \int_A^\infty J_0(kr) \sin(tk) dk, \\ G_u^l(r, t) &\approx \frac{1}{2\pi} \int_0^A k \frac{(\alpha^2 k^2 + \gamma) - (k^2 + 1) + \sqrt{D(k)}}{\sqrt{D(k)} K_2(k)} J_0(kr) \sin(tK_2(k)) dk \\ &\quad + \frac{C}{\pi} \int_A^\infty \frac{J_0(kr)}{k^2} \sin(\alpha tk) dk, \quad \text{with } C = \gamma/\alpha(\alpha^2 - 1) \end{aligned}$$

With the help the integral identity,

$$\int_A^\infty = \int_0^\infty - \int_0^A$$

the expression for G_u^t can be simplified to

$$G_u^t(r, t) \approx G_{0u}^t(r, t) = \frac{\theta(t-r)}{\pi\sqrt{t^2-r^2}}, \quad (\text{A.10})$$

where $\theta(\cdot)$ is the Heaviside step-function and function G_{0u}^t represented by the integral

$$G_{0u}^t(r, t) = \frac{1}{2\pi} \int_0^A k J_0(kr) \left\{ \frac{(\alpha^2 k^2 + \gamma) - (k^2 + 1) + \sqrt{D(k)}}{\sqrt{D(k)} K_1(k)} \sin(tK_1(k)) - \frac{2 \sin(tk)}{k} \right\} dk.$$

The expression for $G_u^l(r, t)$ due to a fast decrease of the integrand can be represented as a sum of two integral with the finite limits

$$G_u^l \approx -\frac{1}{2\pi} \int_0^A k \frac{(\alpha^2 - 1)k^2 + \gamma - 1 - \sqrt{D}}{\sqrt{D}K_2(k)} J_0(kr) \sin(tK_2(k)) dk + \frac{C}{\pi} \int_{+0}^{1/A} J_0\left(\frac{r}{\eta}\right) \sin\left(\frac{\alpha t}{\eta}\right) d\eta \quad (\text{A.11})$$

The fundamental solution is in a sum form, which consists of two terms (A.10) and (A.11). The first function has a sharp front and the second function is represented by a smooth function.

APPENDIX B: DERIVATION OF THE ENERGY FLUX DENSITY

The expression for the density of the energy flux can be found in the following way. Multiply the first equation of the system

$$\psi_{,tt}^x - \alpha^2(\psi_{,xx}^x + m\psi_{,yy}^x + p\psi_{,xy}^x) + \gamma(\psi^x - U_{,x}) = 0, \quad (\text{B.1})$$

$$\psi_{,tt}^y - \alpha^2(\psi_{,yy}^y + m\psi_{,xx}^y + p\psi_{,xy}^y) + \gamma(\psi^y - U_{,y}) = 0, \quad (\text{B.2})$$

$$U_{,tt} - (U_{,xx} + U_{,yy} - \psi_{,x}^x - \psi_{,y}^y) + U = 0 \quad (\text{B.3})$$

by $\psi_{,t}^x$, the second by $\psi_{,t}^y$ and the last by $\gamma U_{,t}$ and rearrange the terms using the relations

$$\psi_{,x}^x U_{,t} = \frac{\partial}{\partial x} (\psi^x U_{,t}) - \frac{\partial}{\partial t} (\psi^x U_{,x}) + \psi_{,t}^x U_{,x}, \quad \psi_{,y}^y U_{,t} = \frac{\partial}{\partial y} (\psi^y U_{,t}) - \frac{\partial}{\partial t} (\psi^y U_{,y}) + \psi_{,t}^y U_{,y},$$

$$\psi_{,xy}^y \psi_{,t}^x = \frac{\partial}{\partial x} (\psi_{,y}^y \psi_{,t}^x) - \psi_{,y}^y \psi_{,xt}^x, \quad \psi_{,xy}^x \psi_{,t}^y = \frac{\partial}{\partial y} (\psi_{,x}^x \psi_{,t}^y) - \frac{\partial}{\partial t} (\psi_{,x}^x \psi_{,y}^y) + \psi_{,y}^y \psi_{,xt}^x.$$

Subsequent summation over the obtained new equations results in the following relation for the energy conservation:

$$\frac{\partial}{\partial t} W + \frac{\partial}{\partial x} S_x + \frac{\partial}{\partial y} S_y = 0, \quad (\text{B.4})$$

where W is the density of energy

$$W = \frac{1}{2} \{ \gamma(U_{,t}^2 + U^2 + (\psi^x - U_{,x})^2 + (\psi^y - U_{,y})^2) + (\psi_{,t}^x)^2 + (\psi_{,t}^y)^2 + \alpha^2 m((\psi_{,x}^x)^2 + (\psi_{,y}^y)^2 + (\psi_{,x}^y)^2 + (\psi_{,y}^x)^2) + \alpha^2 p(\psi_{,x}^x + \psi_{,y}^y)^2 \} \quad (\text{B.5})$$

and S_x, S_y are the components of the vector of the energy flux

$$S_x = U_{,t}(\psi^x - U_{,x}) - \alpha^2 \psi_{,t}^x(\psi_{,x}^x + p\psi_{,y}^y) - \alpha^2 m\psi_{,t}^y \psi_{,x}^y, \quad (\text{B.6})$$

$$S_y = U_{,t}(\psi^y - U_{,y}) - \alpha^2 \psi_{,t}^y(\psi_{,y}^y + p\psi_{,x}^x) - \alpha^2 m\psi_{,t}^x \psi_{,y}^x.$$

For the next step the local rotations $\psi^x(x, y, t)$ and $\psi^y(x, y, t)$ have to be elaborated. According to system (8) for ψ_{nk}^x and ψ_{nk}^y ,

$$\psi_{nk}^x(k, \varphi_k, t) = \frac{P(-i)^{n+1} \gamma J_n(kr_0) k_1}{((k^2 - (\Phi + n\Omega)^2 + 1)(\alpha^2 k^2 - (\Phi + n\Omega)^2 + \gamma) - \gamma k^2)} \exp(in\varphi_k - it(\Phi + n\Omega)),$$

$$\psi_{nk}^y(k, \varphi_k, t) = \frac{P(-i)^{n+1} \gamma J_n(kr_0) k_2}{((k^2 - (\Phi + n\Omega)^2 + 1)(\alpha^2 k^2 - (\Phi + n\Omega)^2 + \gamma) - \gamma k^2)} \exp(in\varphi_k - it(\Phi + n\Omega)).$$

Applying the following inverse Fourier transform to these expressions:

$$\{\psi_n^x, \psi_n^y\}(r, \varphi, t) = \frac{1}{4\pi^2} \int_0^\infty \int_0^{2\pi} k \{\psi_{nk}^x, \psi_{nk}^y\}(k, \varphi_k, t) \exp(ikr \cos(\varphi_k - \varphi)) d\varphi_k dk,$$

gives

$$\psi_n^x = \frac{Q}{2\pi} \int_0^\infty \frac{k^2 (\cos(\varphi) I_c - \sin(\varphi) I_s) J_n(kr_0)}{((k^2 - (\Phi + n\Omega)^2 + 1)(\alpha^2 k^2 - (\Phi + n\Omega)^2 + \gamma) - \gamma k^2)} \exp(in(\varphi - \Omega t)) dk, \quad (\text{B.7})$$

$$\psi_n^y = \frac{Q}{2\pi} \int_0^\infty \frac{k^2 (\cos(\varphi) I_s + \sin(\varphi) I_c) J_n(kr_0)}{((k^2 - (\Phi + n\Omega)^2 + 1)(\alpha^2 k^2 - (\Phi + n\Omega)^2 + \gamma) - \gamma k^2)} \exp(in(\varphi - \Omega t)) dk, \quad (\text{B.8})$$

where

$$Q = -iP \exp(-i\Phi t), \quad I_c = \frac{n}{kr} J_n(kr), \quad I_s = i \frac{\partial J_n(kr)}{k \partial r}.$$

Asymptotic analysis of integrals (A.5) and (B.6) for a large distance from the origin shows that ψ_n^x and ψ_n^y are decreasing as $1/r^\delta$ with $\delta > 1$. Thus, the input of these functions in the energy flux is negligibly small compared to the input of $U(\dots)$ -terms. So, the vector of energy flux can be rewritten as follows $\mathbf{S} = (S_x, S_y) \approx -U_{,t}(U_{,x}, U_{,y})$ or in the co-ordinate-independent form $\mathbf{S} \approx -\rho c_{0t}^3 U_{,t} \nabla U$, where coefficient ρc_{0t}^3 appears for dimensional reason.